Molecular dynamics studies of some carbon nanotubes chiral structures

Moshibudi Shai[1], **Thuto Mosuang**[1], **and Erasmus Rammutla**[1]

[1] Department of Physics & Geology, University of Limpopo, Private Bag x1106, Sovenga, 0727, Polokwane, South Africa

Corresponding author: thuto.mosuang@ul.ac.za

Abstract. Structural and equilibrium properties of armchair (cnt(12,12)) and two chiral (cnt(12,10) and cnt(10,12)) carbon nanotubes are studied using classical molecular dynamics. The formulation uses the Tersoff potential under the NVT ensemble to study these properties. Structural properties are studied using the radial distribution and structure factor functions. The equilibrium properties are studied using the total energy against lattice parameter variation. Similarities and differences in cnt(12,12), cnt(12,10), and cnt(10,12) symmetries are discussed.

1. Introduction

Carbon materials are widely used in various industries because of their exclusive mechanical properties [1]. It is now a known detail that the covalent bonding between carbon-carbon atoms contribute heavily to the strength of tetrahedral diamond bonds and to the in-plane hexagonal bonds. Therefore, carbon nanotubes, which are cylindrical hexagonal arrangements of carbon atoms along one given axis, represent the ideal carbon fibre, which should automatically hold the best mechanical properties [1-4]. This characteristic feature is crucial in the application of nanotubes, given the importance of strong light weight composites. Theoretical calculations have predicted the Bulk modulus B of single walled carbon nanotubes to be in the range of 38 to 191 GPa [5,6] disregarding the chirality. These calculations are based on the bulk modulus of graphite of which experimental measurements give 27-42 GPa [7,8]. Due to minute size effects, most of the experimental works have eluded measurements of the bulk modulus in multi-walled carbon nanotubes (mwcnt). But Young's modulus measurements, which can be described as the stiffness of the mwcnt in one dimension, were performed by Treacy *et al*. [9] to be in the range of ~2.0 TPa. Furthermore, atomic force microscopy techniques were used by Salvetat *et al*. [10] to obtain a Young's modulus of ~1.2 TPa. Measurements of single walled carbon nanotubes (swcnt) can pose a serious challenge due to their small diameters (~1.5 nm) and the fact that swcnt tend to form bundles. In so saying, measuring bundle nanotubes properties may not easily be projected to unit nanotubes and vice versa.

Various theoretical calculations of some small radii carbon nanotubes have focused on their electronic properties. First principles local density functional [11] and empirical tight binding approximations [12] predict that these nanoscale fibres will show conducting properties varying from metallic to semiconducting depending on the radii and chiral symmetry. Apart from these electronic and elastic properties, very little has been reported about their lattice and formation energies. It is such information which could facilitate optimal conditions essential for producing carbon nanotubes with high strength-to-weight ratios [13].

In this study, classical molecular dynamics (MD) is used to investigate the structural and equilibrium properties of swcnt. Structural configurations are extracted from the radial distribution functions and structure factors of the nanotubes. This is worked out at various temperatures in order to observe the flexibility of the potential used. Equilibrium properties are studied through structural optimizations along the a-axis using the Evans NVT ensemble at 300 K temperature and zero pressure. Here total energy is observed with little changes in the a-axis values at constant temperature. The implications of our results are then discussed with reference to earlier experiments and calculations and the accepted graphite and other nanotube results.

2. Computational aspects

Classical MD approach is used to solve the Newton's equations of motion for three types of swcnts discussed in this paper [14]. This MD simulation is performed under the Evans NVT ensemble for both structural and equilibrium properties. The Newtonian equations of motions are integrated using the leapfrog Verlet algorithm with the time step of 1.0×10^{-3} ps. Total energy is averaged after 2000 iterations with equilibration every 200 steps. The interaction between the carbon atoms is described by the well-known Tersoff two-body potentials [15,16]. Tersoff potentials have been used in many carbon and related materials calculations, and have proved that a wide range of structural properties can be determined using this formalism [15,16]. In addition, many studies relating bond length and bond order to total energy and force constants are interpreted correctly, suggesting that this method is a good start in predicting composite properties as discussed in this paper [17-19].

Swcnts modelled in this paper are an armchair (12,12) carbon nanotube, two chiral structures (12,10), and (10,12) nanotubes, thereafter all referred to as cnt(12,12), cnt(12,10), and cnt(10,12) respectively. The structure were chosen such that all have comparable number of carbon atoms; i.e cnt(12,12) has 312 carbon atoms, whilst cnt(12,10) and cnt(10,12) both have 264 and 260 carbon atoms respectively. Furthemore, cnt(12,12) and cnt(12,10) have equal values of *a* and *b*-axis, likewise, for cnt(12,12) and cnt(10,12) the *c*-axis values are equal. Loosely articulating, cnt(12,10) can be thought of as the projection of cnt(12,12) along the *a* and *b*-axis whereas cnt(10,12) can be thought of as the projection of cnt(12,12) along the c-axis. It need to be mentioned that all the literature studied works only with chiral structures of the (2*n*,*n*) form [13,20,21]. The radial distribution functions (***g*(r)**) and structure factors (***S*(k)**) were calculated at 300, 3000, and 5000 K temperature, to observe the behaviour of atomic configurations and interatomic interactions with elevated temperatures. In order to obtain the equilibrium configurations of these models *a*-axis values were varied with total energy at constant temperature of 300 K until a convincing minimum energy is found. Based on the optimized structures and their energies, various equilibrium properties of these models had been extracted.

3. Results and discussion

3.1 *Structural properties*

In order to draw confidence on the empirical bond-order potential, radial distribution functions ***g*(r)** for swcnt in two chiral forms have been calculated. When searching for the minimum of the three symmetry configurations; chiral cnt(10,12) configuration produced a maximum value instead of a minimum, so this symmetry was discontinued from the study. Even though ***g*(r)** gives information only up to the second nearest neighbour, the insight upon the arrangement of carbon atoms in nanotubes can be extracted. This can be quantitatively compared with carbon atoms distribution in graphene and graphite formations. Using the peak positions of ***g*(r)**, the nearest neighbour and the second nearest neighbour carbon atoms in swcnt can be determined. The peak positions appear at 1.45 and 2.50 Å for both armchair cnt(12,12) and chiral cnt(12,10), in good agreement with other theoretical calculations and experiments [22-24]. The radial distribution function for cnt(12,12) at 300, 3000, and 5000 K is shown in figure 1. Detailed information from ***g*(r)** along with experimental results of Boiko *et al*. [23] can be harvested in table 1. Figure 2 displays the structure factor functions (***S*(k)**) for the same cnt(12,12) at 300, 3000, and 5000 K. ***S*(k)** is the Fourier transform of the ***g*(r)** from the real space to the reciprocal space.

Table 1 Quantities calculated from the radial distribution functions. r_1 and r_2 represent first and second nearest neighbour distances. n_1 and n_2 represent the coordination number of atoms in the first and second nearest neighbour distances.

	r_1 (Å)	r_2 (Å)	n_1	n_2
cnt(12,12)	1.45	2.50	4.25	2.70
cnt(12,10)	1.45	2.50	4.35	2.90
Graphite[23]	1.43	2.53	3.30	-

Using a pictorial scrutiny of the ***g*(r)** in figures 1 and 2 and comparison of experimental results in table 1, it appears that the carbon nanotubes tubular structure is robust with cylindrically stable structure even at extremes of temperature. This toughness is comparable to that of diamond according to table 1 standards. Atomic distribution around the first nearest neighbour is uniform in all temperature ranges and it resembles that of diamond according to Kakinoki *et al*. [24] even though the peak positions are for graphite. At second nearest neighbour distance (2.50 Å) coordination is diamond-like at 300 K but becomes more graphitic at 5000 K. Wiggles at 3000 and 5000 K peaks on cnt(12,12) suggest that armchair (figure 3) is not as robust as chiral cnt(12,10).

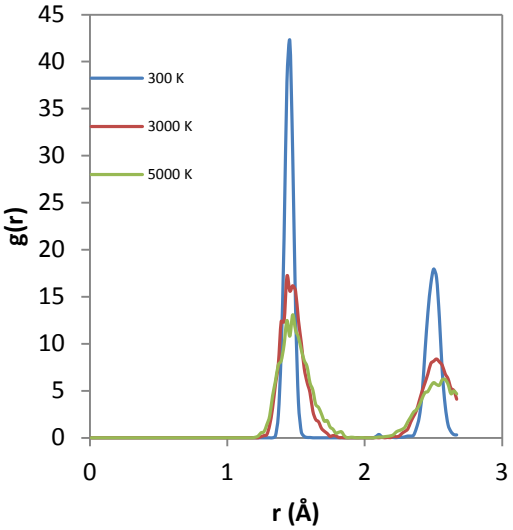

Figure 1. Radial distribution function for the armchair cnt(12,12) configuration at 300, 3000, and 5000 K.

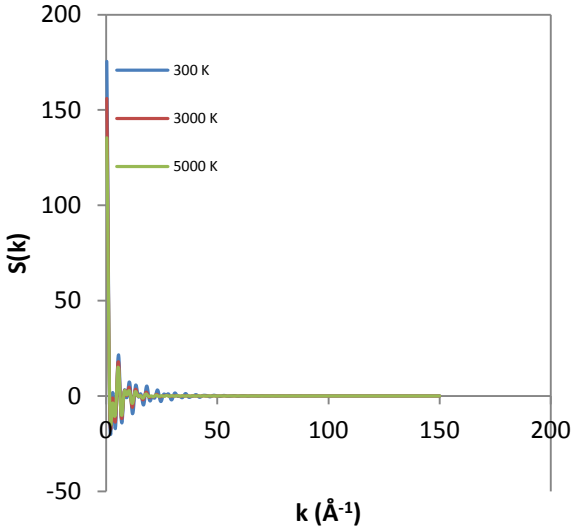

Figure 2. Structure factor functions for the armchair cnt(12,12) configuration at 300, 3000, and 5000 K.

3.2 *Equilibrium properties*

The structural optimization was performed under the Evans NVT ensemble at zero pressure and 300 K temperature. In this environment, equilibrium bundle lattice constant, bulk modulus, bulk modulus derivative, equilibrium energy, and equilibrium volume were calculated. Figures 3 and 4 show how the total energy per atom in nanotube bundles behaves with the varying *a*-axis in both the cnt(12,12) and cnt(12,10) tube bundles. The total energy against *a*-axis data was further least-squares fitted to Murnaghan's [25]equation of state in order to obtain the bulk modulus and its derivative. The results

obtained together with other carbon nanotube calculations [19] and graphite experimental results [7,8] are organized in table 2.

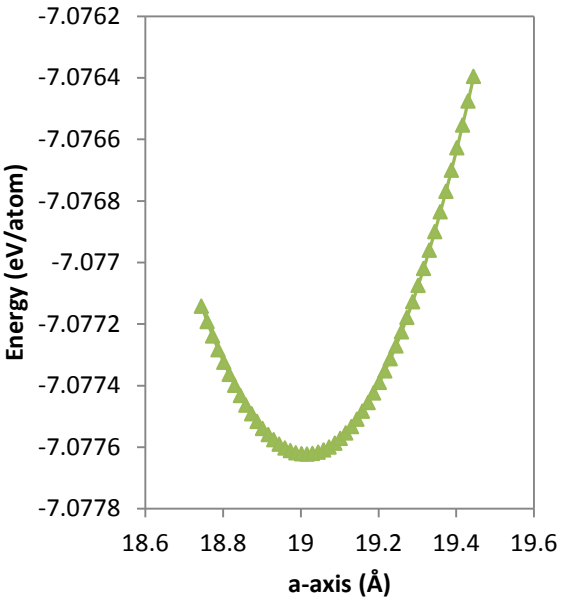

Figure 3. Equilibrium energy as a function of *a*-axis for the armchair cnt(12,12).

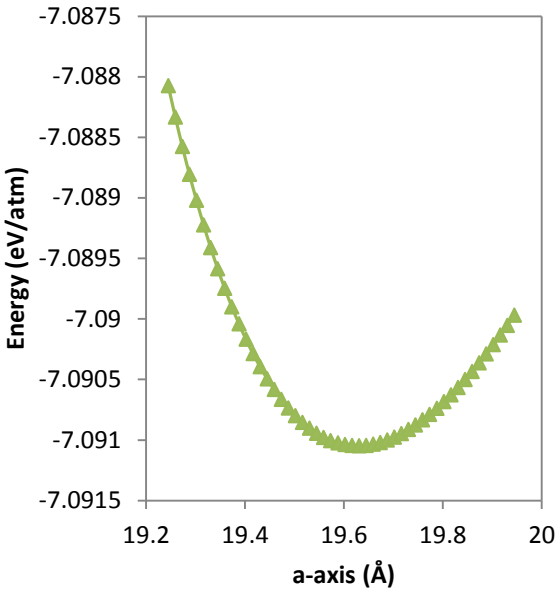

Figure 4. Equilibrium energy as a function of *a*-axis for the chiral cnt(12,10).

The equilibrium lattice constant a for the unit cells of the cnt(12,12) and cnt(12,10) bundles were found to be 19.014 and 19.628 Å for nanotube radii of 8.14 and 7.47 Å respectively. Reich *et al*. [19] demonstrated that the spacing between the tubes in a bundle cannot exceed the graphite equilibrium spacing of 3.35 Å. Applying this concept, tubes with bigger radii will have smaller inter-tubular spacing. To complement this, Tang *et al*. [26] merged x-ray measurements and elasticity theory calculations to show that the wall-to-wall distance between tubes within a bundle may not exceed the graphite equilibrium interlayer spacing. The bulk modulus for the armchair cnt(12,12) and chiral cnt(12,10) were computed to be 21.12 and 44.56 GPa respectively. These results are within the allowed limits of the graphite x-ray measurements of Hanfland *et al*. [7] and Zhao and Spain [8].

Table 2. Calculated lattice constants a, bulk modulus B_0 and its first derivative B', equilibrium energy E_0, and equilibrium volume V_0 of two carbon nanotubes symmetries compared with graphite experimental results [7,8] and calculated results of carbon nanotubes [19].

	cnt(12,12) this work	cnt(12,10) this work	Graphite experiment[7,8]	Nanotubes bundles[19]
a (Å)	19.01	19.63	2.603	11.43
B (GPa)	21.12	44.56	33.80	37.00
B'	1.000	18.37	8.900	11.00
E_0 (eV)	-7.078	-7.091	-	-
V_0 (Å^3)	27.21	28.93	35.12	-

3.3 *Dynamical properties*

Transport properties of carbon ions and even impurities within a tube can be extracted from the simulations using the time-dependent mean square displacement (msd), which is defined by: $\langle r_i^2(t)\rangle = \frac{1}{N}\sum_{i=1}^{N}[r_i(t) - r_i(0)]^2$, where N is the total number of ions in the system, $r_i(0)$, and $r_i(t)$ are initial and advanced position of ions respectively. At elevated temperatures, the carbon ions gain momentum and become highly mobile and so the msd increases with time. The argument can be confirmed by the msd data plotted as function of time for armchair cnt(12,12) and chiral cnt(12,10) configurations as shown in figures 5 and 6.

As it can be seen, at room temperatures, both configurations demonstrate somewhat constant behaviour with time, which suggest that there is no notable carbon ion diffusion. A periodical rise and fall conduct of carbon ions with time at 3000 K is notable to both cnt(12,12) and cnt(12,10). At 5000 K, carbon function in cnt(12,10) increases with increasing time, indicating ion diffusion, whereas oscillatory behaviour is still observed in cnt(12,12). From the slope of carbon ions as function of time in cnt(12,10) at 5000 K, a diffusion coefficient of 0.108 Å^2/ps and a thermal factor of 1.029 Å^2 were computed according to the equation: $\langle r_i^2(t)\rangle = 6Dt + A_0$, where D is the diffusion coefficient and A_0 is some small thermal factor due to atomic vibrations.

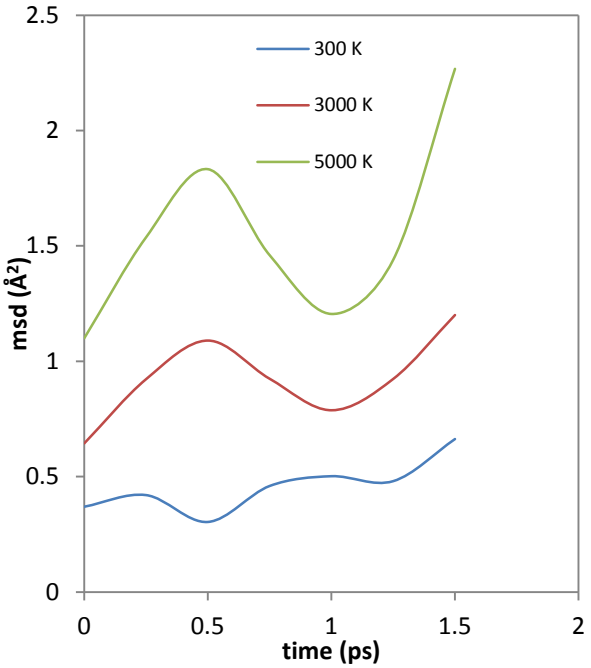

Figure 5. Mean square displacement (msd) of carbon ions in an armchair cnt(12,12) at 300, 3000, and 5000 K.

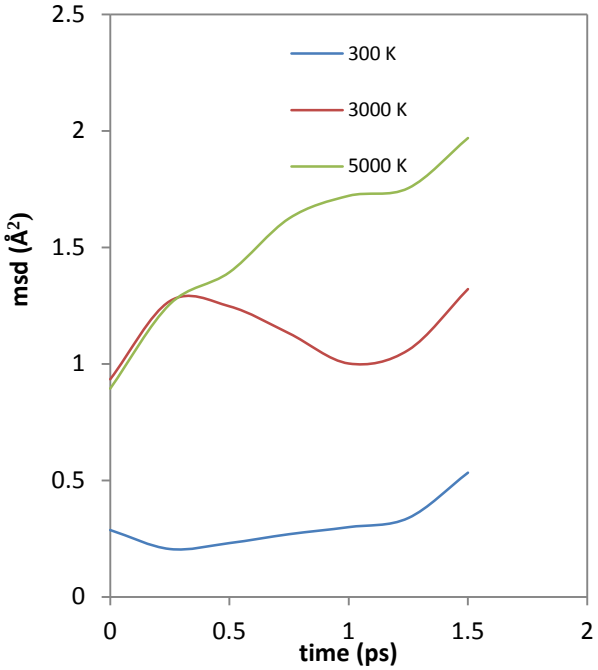

Figure 6. Mean square displacement (msd) of carbon ions in an achiral cnt(12,10) at 300, 3000, and 5000 K.

4. Conclusion

The structural configuration and equilibrium properties of some swcnts symmetry configurations were studied. ***g(r)*** and ***S*(k)** results demonstrate the strength and rigidity of atomic distributions even at extremes of temperature. This in turn validates the flexibility and transferability of the Tersoff potential to nanoscale level. The bulk modulus of the bundles is found to be within the graphite acceptable range. Specifically for cnt(12,12) and cnt(12,10), the larger radius implies smaller bulk modulus and the other way round. The equilibrium volumes are smaller than those of graphite.

Acknowledgements

The UL and IBSA are thanked for financial assistance. CHPC is thanked for computational facilities.

References

[1] Dresselhaus MS, Dresselhuas G, Sugihara K, Spain IL, Goldberg HA 1988 *Graphite Fibers and Filaments* (Springer-Verlag, New York).

[2] Dresselhaus MS, G. Dresselhaus G, and R. Saito R 1995 *Carbon* **33** 883.

[3] Krishnan A, Dujardin E, Ebbesen TW, Yianilos TN, and Treacy MMJ 1998 *Phys. Rev.* B **58** 14013.

[4] Hernández E, Goze C, Bernier P, and Rubio A 1998 *Phys. Rev. Lett.* **80** 4502.

[5] Popov V, Doren VV, and Balkanski M 2000 *Solid State Commun.* **114** 395.

[6] Lu J 1997 *Phys. Rev. Lett.* **79** 1297.

[7] Hanfland M, Beister H, and Syassen K 1989 *Phys. Rev.* B **39** 12598.

[8] Zhao YX and Spain IL 1989 *Phys. Rev.* B **40** 993.

[9] Treacy MMJ, Ebbesen TW, and Gibson TM 1996 *Nature* **381** 680.

[10] Salvetat JP, Bonard JM, Thomson NH, Kulik AJ, Farro L, Bennit W, and Zuppiroli L 1999 *J. Appl. Phys.* A **69** 255.

[11] Mintmire JW, Dunlap BI, and White CT 1992 *Phys. Rev. Lett.* **68** 631.

[12] Hamada N, Sawada S, and Oshiyama A 1992 *Phys. Rev. Lett.* **68** 1579.

[13] Robertson DH, Brenner DW, Mintmire JW 1992 *Phys. Rev.* B **45** 12592.

[14] Smith W, Forester TR and Todorov IT, 2009 *The DL_POLY 2 User Manual,* STFC Daresbury Laboratory, Darebury, Warrington WA4 4AD Cheshire, UK.

[15] Tersoff J 1988 *Phys. Rev.* B **75** 6991.

[16] Tersoff J 1988 *Phys. Rev. Lett.* **61** 2879.

[17] Tersoff J and Ruoff RS 1994 *Phys. Rev. Lett.* **73** 676.

[18] Diao J, Srivastava D, and Menon M 2008 *J. Chem. Phys.* **128** 164708.

[19] Reich S, Thomsen C, and Ordejón P 2002 *Phys. Rev.* B **65** 153407.

[20] Pullen A, Zhao GL, Bagayoko D, and Yang L 2005 *Phys. Rev.* B **71** 205410.

[21] Gao G, Çağin T, and Goddard WA III 1998 *Nanotechnology* **9** 184.

[22] Beeman D, Silverman R, Lynds R, and Anderson MR 1984 *Phys. Rev.* B **30** 870.

[23] Bioko BT, Palatnik LS, and Derevyanchenko AS 1968 *Dokl. Akad. Nauk SSSR* **179** 316 [1968 *Sov. Phys. – Dokl.* **13** 237].

[24] Kakinoki J, Katada K, Hanawa T, and Ino T 1960 *Acta Crystallogr.* **13** 171.

[25] Murnaghan F, 1944 *Proc. Nat. Acad. Sci. USA,* **30** 244.

[26] Tang J, Qin L-C, Sasaki T, Yudasaka M, Matsushita A, Iijima S 2000 *Phys. Rev. Lett.* **85** 1887.